



Optics Letters

Gas spectroscopy through multimode self-mixing in a double-metal terahertz quantum cascade laser

Y. J. HAN,^{1,*} J. PARTINGTON,¹ R. CHHANTYAL-PUN,¹ M. HENRY,² O. AURIACOMBE,² T. RAWLINGS,² L. H. LI,¹ J. KEELEY,¹  M. OLDFIELD,² N. BREWSTER,² R. DONG,¹ P. DEAN,¹ A. G. DAVIES,¹  B. N. ELLISON,² E. H. LINFIELD,¹ AND A. VALAVANIS¹ 

¹School of Electronic and Electrical Engineering, University of Leeds, Leeds LS2 9JT, UK

²Rutherford Appleton Laboratory, STFC, Harwell Oxford, Didcot OX11 0QX, UK

*Corresponding author: y.han@leeds.ac.uk

Received 31 August 2018; revised 10 October 2018; accepted 10 October 2018; posted 7 November 2018 (Doc. ID 344578); published 4 December 2018

A multimode self-mixing terahertz-frequency gas absorption spectroscopy is demonstrated based on a quantum cascade laser. A double-metal device configuration is used to expand the laser's frequency tuning range, and a precision-micromachined external waveguide module is used to enhance the optical feedback. Methanol spectra are measured using two laser modes at 3.362 and 3.428 THz, simultaneously, with more than eight absorption peaks resolved over a 17 GHz bandwidth, which provide the noise-equivalent absorption sensitivity of $1.20 \times 10^{-3} \text{ cm}^{-1} \text{ Hz}^{-1/2}$ and $2.08 \times 10^{-3} \text{ cm}^{-1} \text{ Hz}^{-1/2}$, respectively. In contrast to all previous self-mixing spectroscopy, our multimode technique expands the sensing bandwidth and duty cycle significantly.

Published by The Optical Society under the terms of the [Creative Commons Attribution 4.0 License](https://creativecommons.org/licenses/by/4.0/). Further distribution of this work must maintain attribution to the author(s) and the published article's title, journal citation, and DOI.

<https://doi.org/10.1364/OL.43.005933>

In the terahertz (THz) frequency range, many polar molecules have characteristic spectra arising from transitions between rotational quantum levels. These unique spectral signatures can be used for gas identification and analysis, which makes THz spectroscopy of increasing interest in many fields, including trace gas sensing, environmental monitoring, astronomy, medicine, and security [1,2]. Quantum cascade lasers (QCLs) are important sources within the 2–5 THz range [3–5], with merits including their compact size, coherence, narrow linewidth, tunable emission frequency, and high output power [6–8]. Based on THz QCLs, heterodyne radiometry and direct-transmission gas spectroscopy have been demonstrated [9–11], with their resolution and detectivity improved by phase locking, frequency modulation, and photoacoustic techniques [12–14]. Until recently, these spectroscopy schemes

have required a separate detector or mixer, as well as frequency calibration instrumentation, which increase the complexity and cost of the system. In order to overcome these challenges, a THz gas spectroscopy technique based on self-mixing (SM) in a QCL has been demonstrated [15]. SM interference occurs between the internal and backscattered optical fields in a laser cavity. This induces changes to the terminal voltage, which are sensitive to the amplitude and phase of the reflected radiation, thus enabling the laser device to act both as a radiation source and as a coherent detector [16,17]. This technique removes the need for additional detectors and enables fast detection and self-calibration [18,19]. However, the spectral bandwidth of these SM spectroscopy systems has so far been limited by the <2 GHz tuning range of the single-mode QCLs used in previous works. Here we present a new technique, which exploits the ability of SM systems to monitor the full emission spectrum of their own laser sources, and demonstrate the measurement of methanol spectral features, simultaneously, from two modes of a multimode THz QCL over a 17 GHz range.

The QCL used in this Letter was processed using a gold-gold double-metal (DM) waveguide configuration. The active region is based on a phonon-enhanced bound-to-continuum design. The layer sequence of an active module in nanometers is **3.7/10.5/0.5/12.2/1/12.5/1.9/11/2.8/8.8/2.8/7.9/2.8/6.6/2.8/_15.8/2.8/13.8**, where the $\text{Al}_{0.15}\text{Ga}_{0.85}\text{As}$ barriers are shown in bold, and the doping density in the underlined GaAs well is $3.4 \times 10^{16} \text{ cm}^{-3}$. The details of the device fabrication have been described elsewhere [20]. In order to increase the reinjection efficiency of the optical feedback, the device was integrated into a micro-machined waveguide block. Two halves of an overmoded $300 \times 150 \mu\text{m}^2$ rectangular waveguide with a diagonal feedhorn were machined into a pair of copper blocks. A standalone chip with $60 \times 980 \mu\text{m}^2$ QCL ridges was indium-soldered into a recess of one half-block; then the other half-block was fixed to form the completed rectangular waveguide and diagonal feedhorn assemblies [21].

The optical configuration of the spectroscopy system is similar to that in Ref. [19] and is illustrated in Fig. 1. The emitted radiation from the QCL was directed through a 96.5 cm long gas cell and was reflected back using a mechanically adjustable optical delay line into the QCL along the same optical path. The SM perturbations to the QCL voltage were measured as a function of the optical delay time, and a fast Fourier transform (FFT) was used to infer the full-band emission spectrum of the QCL. A dry mechanical pump was used to evacuate the gas cell resulting in a base pressure of 0.03 Torr. A high purity methanol sample was degassed and evaporated into the gas cell to the desired pressure measured by a capacitance manometer (MKS α -Baratron AA01).

The optical delay time was controlled using a Newport ILS-200 motor translation stage, with a speed of 100 mm/s, a step size of 1 μm , and a maximum distance of 200 mm. The maximum round-trip delay $D = 800$ mm (using beam-folding optics as in Fig. 1) corresponds to a FFT sampling resolution ($\Delta f = c/D$, c is the speed of light) of around 375 MHz, and the step size $\Delta l = 1$ μm corresponds to a FFT spectral bandwidth ($f_{\text{fold}} = f_s/2 = c/(8\Delta l)$, f_s is the sampling frequency) of 37 THz.

Emission spectra of the QCL were measured at a temperature of 10 K, with the gas cell under vacuum. The dc driving current was kept constant for each interferogram, and the spectra in the full dynamic range were obtained by stepping the current at a range from 110 to 245 mA. As shown in Fig. 2, multimode emission was obtained with two main emissions around 3.362 (mode A) and 3.428 THz (mode B) being observed simultaneously across the full dynamic range. Several lower-intensity side modes were also observed around the main emission lines over limited current ranges. Effective refractive indices of 4.046 and 4.036 were calculated for the side modes around the 3.362 and 3.428 THz lines, respectively, indicating that they originate from lateral confinement. To estimate the frequency evolution of the two main modes, the emission frequencies are plotted in Fig. 3 as a function of the current. The peak frequencies were obtained by using a Gaussian fit to the measured spectra. As the current was increased, both laser modes were shown to have a redshift with the frequency tuning ranges around 10 GHz in each case: from 3.3696–3.3594 THz (mode A) and 3.4354–3.4253 THz (mode B), respectively. Both tuning curves can be divided into three piecewise-linear segments. This gives tuning rates of –380,

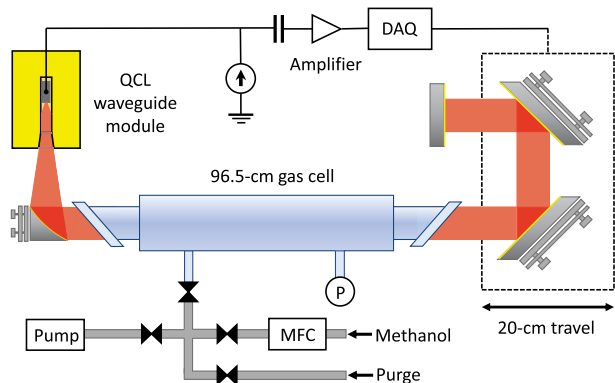


Fig. 1. Schematic illustration of the gas spectroscopy system. P, pressure gauge; MFC, mass flow controller.

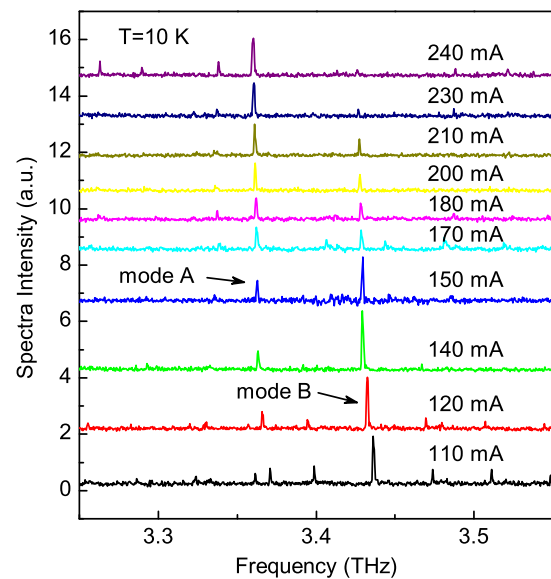


Fig. 2. Emission spectra of a THz QCL as a function of the dc drive current, measured through self-mixing interferometry at 10 K and with the gas cell under vacuum.

–173, and –31 MHz/mA for mode A, and –340, –171, and –34 MHz/mA for mode B, respectively.

During the measurement, data were recorded with the translation stage moving in forward or reverse directions to reduce data acquisition time, and 10 scans were averaged for every current step to decrease noise. A current-sweep step of 1.0 mA was used in Fig. 3. As such, a data acquisition rate of 0.05 samples/s was obtained, giving a total scan time of 2720 s to sweep the whole current range. The frequencies in Fig. 3 exhibit small

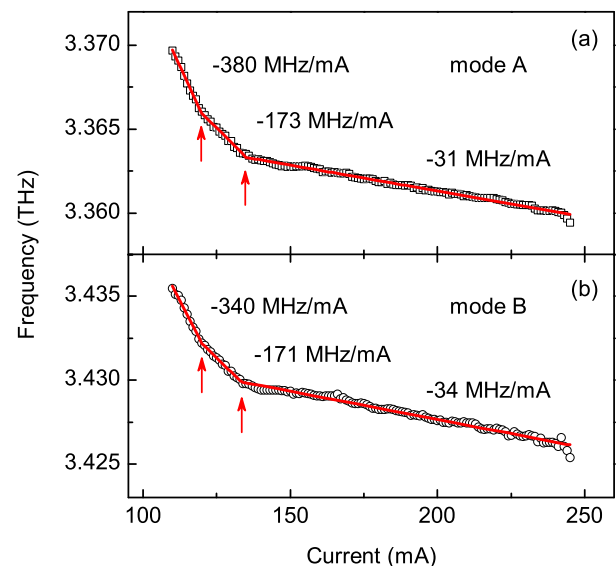


Fig. 3. Frequency of the two highest intensity laser modes, (a) mode A and (b) mode B, measured at 10 K with the gas cell under vacuum, as a function of the drive current. The black squares and circles are the measured data; the red solid lines are the linear fits to the experiment data; and the red arrows indicate the separate points of the piecewise-linear segments.

fluctuations less than 200 MHz when the current is higher than 135 mA, only half of the frequency resolution of the system. Thus, this small frequency perturbation is neglected during the data processing. Based on our previous measurements [17,19], our spectroscopy system is estimated to operate in the weak feedback regime ($C < 1$), but it would also work in the moderate feedback regime [18].

We assume that different laser modes operate independently in the Fabry–Perot resonator of the QCL. In the case of weak feedback, the SM-induced voltage modulation amplitude can be given by the sum of the contributions from all the individual laser modes [15,19], using

$$U_{SM} \propto \sum_i T_i \cos(2\pi\nu_{0i}\tau_i), \quad (1)$$

where i is the index of laser mode, T_i is a single-pass Beer–Lambert power transmission factor, ν_{0i} is the unperturbed laser mode frequency, and τ_i is the external cavity round-trip time. The laser mode intensity obtained from the SM interferogram is proportional to the corresponding power transmission factor. With the assistance of the integrated *in situ* frequency monitoring scheme, the transmission spectra of gases, therefore, can be measured by sweeping the mode frequencies of the QCLs, with and without the gas present within the cell, and the gas absorption coefficient, α , can be calculated using the familiar Beer–Lambert law:

$$\alpha = -\ln(A/A_0)/L_{\text{cell}}, \quad (2)$$

where A and A_0 are the respective amplitude of the transmission spectra with and without gas in the cell, and L_{cell} is the length of the gas cell. Note that the transmission spectra can be obtained simultaneously for all the laser modes by using this approach, which is much more efficient than SM spectroscopy based on single-mode lasers.

To demonstrate the validity of this approach, the emission frequency and intensity of the two laser modes were measured over the full dynamic current range with and without methanol vapor in the cell. Figure 4 shows the normalized transmission spectra of 5.0 Torr methanol. The use of a multimode QCL yielded a total measurement bandwidth of 17 GHz, much wider than the 2 GHz obtained using a single-mode QCL [15,19]. As such, eight absorption peaks and one absorption band were resolved. For comparison, the spectra were simulated based on data in the JPL molecular spectroscopy catalog [22], using a Voigt profile to account for self-broadening and Doppler broadening [19]. A small frequency offset between the measured and simulated spectra was observed, which could be attributed to a calibration offset in the motion controller. With a correction of -0.6 GHz (0.02%), the measured spectra agree well with the catalogued data. The absorption peaks of methanol at 3.3597, 3.3616, 3.3629, and 3.4282 THz are relatively well resolved. With lower pressure and a smaller current scanning step, more peaks could potentially be resolved within the broad absorption band around 3.3685 THz.

The pressure-dependent methanol transmission spectra are shown in Fig. 5 for the absorption peaks at 3.3616 and 3.4282 THz, which are the strongest features detected using each laser mode. The absorption at 3.3616 THz is strong, and the unsaturated transmission spectra can be obtained only at pressures lower than 1.0 Torr. For the weak absorption at 3.4282 THz, pressures higher than 5.0 Torr are needed to

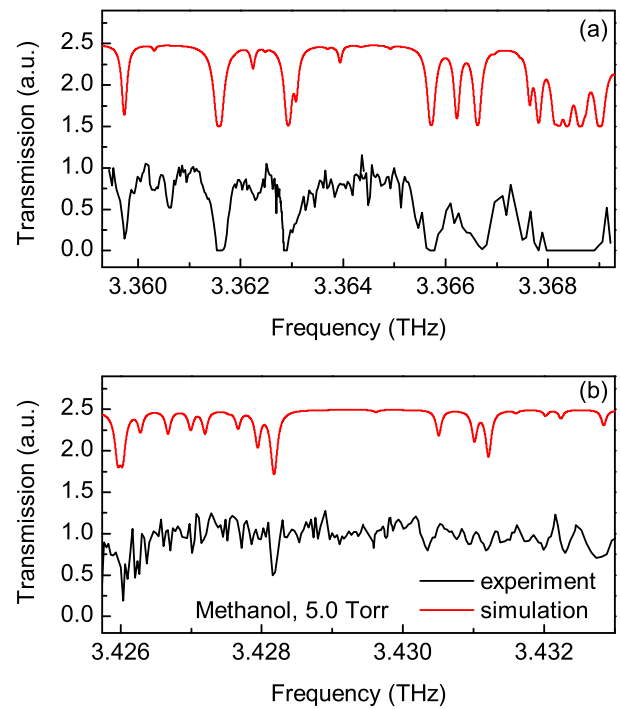


Fig. 4. Transmission spectra of 5.0 Torr methanol, measured with (a) laser mode A and (b) laser mode B, simultaneously. The red lines are the calculated spectra (+1.5 a.u.) based on the data from the JPL molecular spectroscopy catalog [22], and the black lines are the measured results.

acquire measurable signals. With increasing gas pressure, the transmission decreases around both absorption peaks, and the spectral lines become broader. When the pressure is lower than

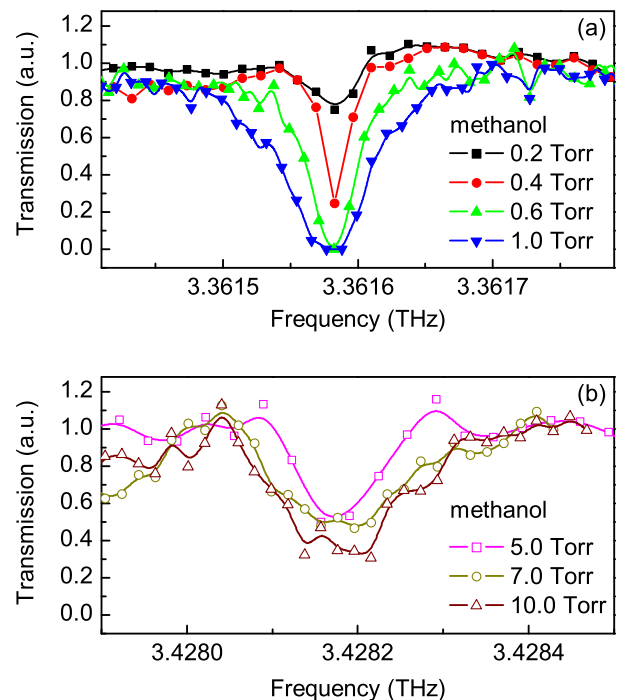


Fig. 5. Transmission spectra of methanol as a function of vapor pressure, measured with (a) laser mode A and (b) laser mode B, respectively.

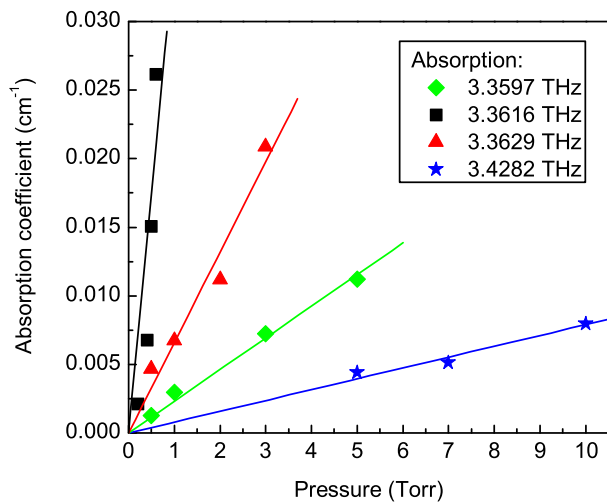


Fig. 6. Coefficient of different absorption bands as a function of methanol vapor pressure. The solid lines show the linear fits to the data points.

1.0 Torr, the linewidth of the spectra only vary slightly with increasing pressure, without showing a clear pressure broadening effect. This can be ascribed to Doppler broadening and limited spectral resolution. This could potentially be mitigated through higher resolution measurements of the frequency pulling effects. Based on the transmission spectra, the coefficients of the principal absorption lines were calculated using Eq. (2). As shown in Fig. 6, the absorption coefficients increase linearly with increasing methanol vapor pressure, and their transition moment is proportional to the slopes. This linear response, as expected from the Beer–Lambert law, can be used to determine the absolute concentration of the gas.

To assess the sensitivity of our SM approach, the noise-equivalent absorption sensitivity (NEAS) was calculated using the following equation:

$$\text{NEAS} = \frac{\Delta P}{P_0} \frac{1}{L_{\text{eff}}} \frac{1}{\sqrt{B/n}}, \quad (3)$$

where $\Delta P/P_0$ is the intensity noise on the baseline without any absorber, L_{eff} is the effective interaction length, B is the detection bandwidth, and n is the number of the scans. For our measurement, $\Delta P/P_0$ is taken as the standard deviation of the baseline transmission, $B = 0.5$ Hz, and $n = 10$. The NEAS is $1.20 \times 10^{-3} \text{ cm}^{-1} \text{ Hz}^{-1/2}$ and $2.08 \times 10^{-3} \text{ cm}^{-1} \text{ Hz}^{-1/2}$ for the methanol absorption at 3.3616 and 3.4282 THz, respectively.

In summary, broadband THz gas spectroscopy has been demonstrated using SM interferometry in a multimode THz QCL for the first time, to the best of our knowledge. The transmission spectra of methanol were simultaneously obtained within two distinct frequency ranges from 3.359 to 3.369 THz and from 3.426 to 3.433 THz. This approach has increased the total measurement bandwidth obtainable using a QCL-based SM scheme by a factor of ~ 7 and underpins future work to develop the first broadband “detector-free” multi-gas QCL spectroscopy systems.

Funding. UK Centre for Earth Observation Instrumentation (CEOI) (RP10G0435A03); European Space Agency (ESA) (GSTP 4000114487/15/NL/AF); Royal Society (WM150029); Engineering and Physical Sciences Research Council (EPSRC) (EP/J017671/1, EP/P021859/1); H2020 European Research Council (ERC) (THEMIS 727541).

Acknowledgment. The data associated with this Letter are openly available from the University of Leeds data repository: <https://doi.org/10.5518/436>.

REFERENCES

1. M. Tonouchi, *Nat. Photonics* **1**, 97 (2007).
2. J. B. Baxter and G. W. Guglietta, *Anal. Chem.* **83**, 4342 (2011).
3. R. Köhler, A. Tredicucci, F. Beltram, H. E. Beere, E. H. Linfield, A. G. Davies, D. A. Ritchie, R. C. Iotti, and F. Rossi, *Nature* **417**, 156 (2002).
4. C. Walther, M. Fischer, G. Scalari, R. Terazzi, N. Hoyler, and J. Faist, *Appl. Phys. Lett.* **91**, 131122 (2007).
5. M. Wienold, B. Roben, X. Lü, G. Rozas, L. Schrottke, K. Biermann, and H. T. Grahn, *Appl. Phys. Lett.* **107**, 202101 (2015).
6. A. Barkan, F. K. Tittel, D. M. Mittleman, R. Dengler, P. H. Siegel, G. Scalari, L. Ajili, J. Faist, H. E. Beere, E. H. Linfield, A. G. Davies, and D. A. Ritchie, *Opt. Lett.* **29**, 575 (2004).
7. Q. Qin, J. L. Reno, and Q. Hu, *Opt. Lett.* **36**, 692 (2011).
8. L. H. Li, L. Chen, J. R. Freeman, M. Salihi, P. Dean, A. G. Davies, and E. H. Linfield, *Electron. Lett.* **53**, 799 (2017).
9. J. R. Gao, J. N. Hovenier, Z. Q. Yang, J. J. A. Baselmans, A. Baryshev, M. Hajenius, T. M. Klapwijk, A. J. L. Adam, T. O. Klaassen, B. S. Williams, S. Kumar, Q. Hu, and J. L. Reno, *Appl. Phys. Lett.* **86**, 244104 (2005).
10. H. Richter, A. D. Semenov, S. G. Pavlov, L. Mahler, A. Tredicucci, H. E. Beere, D. A. Ritchie, K. S. Il'in, M. Siegel, and H.-W. Hübers, *Appl. Phys. Lett.* **93**, 141108 (2008).
11. H.-W. Hübers, R. Eichholz, S. G. Pavlov, and H. Richter, *J. Infrared Millim. Terahertz Waves* **34**, 325 (2013).
12. Y. Ren, D. J. Hayton, J. N. Hovenier, M. Cui, J. R. Gao, T. M. Klapwijk, S. C. Shi, T. Y. Kao, Q. Hu, and J. L. Reno, *Appl. Phys. Lett.* **101**, 101111 (2012).
13. R. Eichholz, H. Richter, M. Wienold, L. Schrottke, R. Hey, H. T. Grahn, and H.-W. Hübers, *Opt. Express* **21**, 32199 (2013).
14. P. Patimisco, S. Borri, A. Sampaolo, H. E. Beere, D. A. Ritchie, M. S. Vitiello, G. Scamarcio, and V. Spagnolo, *Analyst* **139**, 2079 (2014).
15. T. Hagelschuer, M. Wienold, H. Richter, L. Schrottke, K. Biermann, H. T. Grahn, and H.-W. Hübers, *Appl. Phys. Lett.* **109**, 191101 (2016).
16. T. Taimre, M. Nikoli, K. Bertling, Y. L. Lim, T. Bosch, and A. D. Raki, *Adv. Opt. Photonics* **7**, 570 (2015).
17. J. Keeley, J. Freeman, K. Bertling, Y. L. Lim, R. A. Mohandas, T. Taimre, L. H. Li, D. Indjin, A. D. Raki, E. H. Linfield, A. G. Davies, and P. Dean, *Sci. Rep.* **7**, 7236 (2017).
18. T. Hagelschuer, M. Wienold, H. Richter, L. Schrottke, H. T. Grahn, and H.-W. Hübers, *Opt. Express* **25**, 30203 (2017).
19. R. Chhantyal-Pun, A. Valavanis, J. T. Keeley, P. Rubino, I. Kundu, Y. J. Han, P. Dean, L. H. Li, A. G. Davies, and E. H. Linfield, *Opt. Lett.* **43**, 2225 (2018).
20. Y. J. Han, L. H. Li, A. Valavanis, N. Brewster, J. X. Zhu, R. Dong, P. Dean, L. Bushnell, M. Oldfield, A. G. Davies, B. N. Ellison, and E. H. Linfield, in *Proceedings of THz for CBRN and Explosives Detection and Diagnosis*, M. F. Pereira, ed. (Springer, 2017), pp. 123–134.
21. A. Valavanis, M. Henry, Y. J. Han, O. Auriacombe, R. Dong, T. Rawlings, L. H. Li, M. Oldfield, N. Brewster, A. G. Davies, B. N. Ellison, and E. H. Linfield, *Presented at the IRMMW-THz*, Copenhagen, Denmark, September 25–30, 2016.
22. H. M. Pickett, R. L. Poynter, E. A. Cohen, M. L. Delitsky, J. C. Pearson, and H. S. P. Müller, *J. Quant. Spectrosc. Radiat. Transfer* **60**, 883 (1998).